Title

In vivo and in vitro sustained release of ranibizumab from a nanoporous thin-film device.

Permalink

https://escholarship.org/uc/item/32n2v88w

Journal

Drug delivery and translational research, 6(6)

ISSN

2190-393X

Authors

Lance, Kevin D
Bernards, Daniel A
Ciaccio, Natalie A
et al.

Publication Date

2016-12-01

DOI

10.1007/s13346-016-0298-7

Peer reviewed

CrossMark

ORIGINAL ARTICLE

In vivo and in vitro sustained release of ranibizumab from a nanoporous thin-film device

Kevin D. Lance[1] · Daniel A. Bernards[2] · Natalie A. Ciaccio[2] · Samuel D. Good[3] ·
Thaís S. Mendes[3] · Max Kudisch[3] · Elliot Chan[3] · Mynna Ishikiriyama[3] ·
Robert B. Bhisitkul[3] · Tejal A. Desai[1,2]

Abstract Current administration of ranibizumab and other therapeutic macromolecules to the vitreous and retina carries ocular risks, a high patient treatment burden, and compliance barriers that can lead to suboptimal treatment. Here we introduce a device that produces sustained release of ranibizumab in the vitreous cavity over the course of several months. Composed of twin nanoporous polymer thin films surrounding a ranibizumab reservoir, these devices provide release of ranibizumab over 16 weeks in vitro and 12 weeks in vivo, without exhausting the initial drug payload. Following implantation in vivo, devices were well-tolerated and showed no sign of immune response. This platform presents a potential solution to the challenge of delivering protein therapeutics to the vitreous and retina for sustained periods of time.

Keywords Nanoporous · Drug delivery · Biodegradable · Controlled release · Ranibizumab · Sustained release

Introduction

The primary routes of drug delivery for eye diseases are topical drops and intraocular injections. Topical administrations

✉ Tejal A. Desai
  tejal.desai@ucsf.edu

[1] UC Berkeley - UCSF Graduate Group in Bioengineering, 1700 4th Street, QB3 Byers Hall, Room 203, San Francisco, CA 94158, USA

[2] Department of Bioengineering and Therapeutic Sciences, University of California San Francisco, San Francisco, CA 94158, USA

[3] Department of Ophthalmology, University of California San Francisco, 400 Parnassus Ave, 7th Floor, San Francisco, CA 94143, USA

have sustained prominence due to their simplicity and minimal invasiveness. Unfortunately, compliance and persistence are known issues with this route of administration, and clinically proven therapies lose efficacy in real world patient populations [1, 2]. Furthermore, treating retinal diseases with topical drops is rare given that the permeability of therapeutics is typically insufficient to achieve a therapeutic concentration at the targeted site [3–5]. With the introduction of ocular anti-vascular endothelial growth factor (VEGF) agents to treat age-related macular degeneration (AMD), intraocular injection became a widespread technique for administration of therapeutic proteins for retinal disease. Following first-in-class ranibizumab (Lucentis, Genentech, Inc., South San Francisco, CA), the off-label use of bevacizumab (Avastin, Genetech, Inc. South San Francisco, CA) and the approval of aflibercept (Eylea, Regeneron, Inc., Tarrytown, NY) have diversified the landscape of retinal therapies, and expanded approved disease indications [6–9]. With chronic diseases, such as AMD, repeated injections increase the long-term likelihood of an injection-induced trauma or reaction [10]. In addition, the increased patient load places a notable strain on clinicians that may become unsustainable with current treatment regimens [11, 12]. So despite the effectiveness of intraocular injection, its invasiveness, cost of therapy, and impact on clinicians has led to alternative protocols to reduce treatment frequency [13]. As a consequence, these challenges have spurred substantial development over the past decade to improve intraocular therapeutic delivery [14, 15].

Currently, injectable ocular devices are capable of sustained delivery of only small molecule therapeutics over the course of several months. Ozurdex® is a device that utilizes degradable poly(lactic-co-glycolic acid) (PLGA) to avoid accumulation of devices in the eye upon repeated administration [16, 17]. Iluvien® is a further device iteration that employs a non-degradable device that is capable of

Springer

772

Drug Deliv. and Transl. Res. (2016) 6:771–780

achieving relatively constant release rates that gradually slow as the drug payload is expended [18]. Release can be achieved for up to 3 years, but the carrier material remains resident in the eye after the payload is released. Iluvien® and Ozurdex® are both free-floating implants that may migrate in some patients, but techniques exist to reposition a device and generally complications associated with this were minimal [19–21]. Such injectable devices have made major steps to reduce the invasiveness of intraocular delivery, but these technologies were developed around delivery of small molecules and have lacked extension to biologic, large molecule therapies. Consequently, a host of devices seek to address this under-served area [14, 22, 23].

Particle-based drug carriers remain a popular approach to improve therapies because of their capacity to be injected, and unique strategies have been utilized to accommodate biologics [24, 25]. Biosilicon particles are being investigated for sustained release of bevacizumab from an injectable technology [26]. Therapeutic is adsorbed onto the particles, and drug release and particle degradation can be modulated based on the surface geometry employed. While controlled release has been achieved with these materials, long duration delivery has not been fully vetted. Alternatively, hydrogel particles formed using the proprietary "particle replication in non-wetting templates" (PRINT) process are being developed for delivery of bevacizumab. Release from hydrogel PRINT particles has been demonstrated through 60 days [27], an improvement relative to contemporary ranibizumab injections. For both technologies, particles may migrate within the eye, and in the case of an adverse event, repositioning devices or removing them may prove to be impractical given their small, distributed nature.

Utilizing a depot approach, ForSight Vision4 is developing a port delivery system (PDS) that employs a reservoir with a subconjunctival port to refill the device with large molecule therapeutics as needed. The PDS device is inserted through the sclera at the pars plana, so device migration is not a concern. The external refill port is positioned under the conjunctiva, accessible for refill injections performed at intervals in the clinic. A preliminary study enrolled 20 patients and demonstrated good efficacy through 12 months, yet a number of adverse effects were observed, including endophthalmitis, vitreous hemorrhage, and traumatic cataract [28]. A potential drawback of a depot technology is the possibility of protein stability issues inside of the depot. Non-covalent aggregation and fragmentation by peptide bond hydrolysis can occur in the acidic environments of PLGA depots; therefore, care must be taken to reduce degradation by both careful payload formulation and device fabrication from a polymer that does not rapidly acidify its environment [29, 30].

Among the technologies being developed for intravitreal delivery of large molecule therapeutics, there is an unmet need for an injectable and degradable device capable of long-term release. Nanostructured membranes are one method capable of constant-rate release profiles in vitro and can achieve sustained release over the course of several months [31, 32]. These membranes contain pores with dimensions comparable to the drug molecule size and allow constant-rate release. The membranes are anisotropic, with one side having nanopores (diameter 22.0 ± 10.5 nm) and the opposite side having micropores (diameter 0.54 ± 0.32 μm) [32]. The nanostructured membrane fabrication processes were designed for compatibility with a variety of polymers, but the degradation properties of poly(caprolactone) (PCL) are advantageous for this device technology. PCL is a biodegradable polymer that has the property of maintaining physical structure throughout the majority of its degradation: this enables nanostructure-controlled release rates to last for the duration of the drug payload. In addition, nanostructured PCL films have shown biocompatibility in the eye, and their flexibility as thin films allow them to be furled in an injection device [33, 34].

In this report, a nanostructured biodegradable thin-film device was employed for sustained delivery of ranibizumab into the vitreous cavity. Devices were evaluated for sustained ranibizumab release in vitro for 16 weeks and in vivo for 12 weeks. To allow accurate measurement in vitro and in vivo, ranibizumab was fluorescently tagged with fluorescein. In vitro release gave an average initial release rate of 1.82 μg/day and an average terminal release rate of 0.56 μg/day. To account for device-to-device variation, individual device performance was characterized in vitro prior to introduction into the eye of a New Zealand White rabbit model, where vitreous levels were measured through 12 weeks. Ranibizumab concentrations of 0.83 μg/mL in the vitreous were attained at 12 weeks, and no adverse effects were associated with device residence outside of implantation trauma. Scanning electron microscopy and quartz crystal microbalance (QCM) were both utilized to investigate protein adsorption onto device surfaces, which was shown to be minute. This demonstrates the potential to encapsulate and release protein therapeutics from such devices over sustained durations.

Materials and methods

Materials

Polycaprolactone (80 kDa, Mn), 2,2,2-trifluoroethanol, potassium phosphate monobasic and dibasic, and polysorbate 20 were obtained from Sigma-Aldrich (St. Louis, MO). Polydimethylsiloxane, sodium carbonate, sodium bicarbonate, and L-histidine were obtained from Thermo Fisher Scientific (Waltham, MA). D-(+)-trehalose was obtained from VWR International, Inc. (Radnor, PA). Ranibizumab (Lucentis®, Genentech, South San Francisco, CA) was obtained from the UCSF Department of Ophthalmology.

Drug Deliv. and Transl. Res. (2016) 6:771–780

773

FITC-ranibizumab preparation

FITC-ranibizumab was prepared with a FluoroTag fluorescein isothiocyanate Conjugation Kit (Sigma-Aldrich). Briefly, ranibizumab was dialyzed (Slide-A-Lyzer Dialysis Cassette, 10,000 MWCO, Life Technologies, Waltham, MA) in a 0.1 M carbonate buffer (pH 9) and subsequently reacted with the FluoroTag FITC conjugation kit. The product was dialyzed again in a formulation buffer of 10 mM histidine HCl, 292 mM trehalose, and 0.01 % polysorbate 20, at pH 5.5) and then lyophilized with an AdVantage 2.0 BenchTop Freeze Dryer/Lyophilizer (SP Scientific, Warminster, PA). The resulting formulation used in this study was 6.8 % (w/w) ranibizumab. All results reflect the mass of pure ranibizumab, not the mass of the total formulation.

Device fabrication

Thin films of nanoporous PCL were fabricated as described previously [32]. In brief, zinc oxide nanowires were used as a template to define nanopores in a thin layer of PCL that is supported by a thicker microporous layer. Devices were fabricated by sealing the perimeter of two 10-mm diameter, circular PCL films around a 3-mm diameter pellet of FITC-ranibizumab (Fig. 1a). A poly(dimethylsiloxane) (Sylgard, 184, Dow Corning, NY) slab was used as a base support, and heat and pressure were applied by a 70 °C hollow cylinder of heated metal for 5 s to fuse the two nanoporous PCL films together. Ice-cold water was introduced to the center of the metal cylinder to prevent excessive heating of the films after 5 s.

Scanning electron microscopy

Nanoporous thin film and device morphology was examined by scanning electron microscopy at the device surface and in cross-section. PCL films and device fragments were cross-sectioned by freeze-fracture in liquid nitrogen. Devices were coated with an 8 nm layer of Au/Pd by a Cressington-HR sputter coater and imaged with a Carl Zeiss Ultra 55 field emission scanning electron microscope using an Everhart-Thornley secondary electron detector.

In vitro elution experiments

Device performance was evaluated in vitro by drug elution in 2 mL phosphate-buffered saline (PBS) at pH 7.4 as elution media. Elution studies were performed at 37 °C with continuous shaking on an orbital shaker for 16 weeks. Sampling with complete replacement of media was performed at weekly intervals. Twenty-two devices were used for long-term in vitro release studies. FITC-ranibizumab concentration in the elution media was measured by plate fluorometer (Fluorocount, Packard Biosciences (PerkinElmer), Waltham, MA), except where high performance size exclusion chromatography was used to assay drug aggregation. Results are reported as plus/minus their standard deviations.

In vivo elution experiments

Prior to in vivo implantation, devices were tested for release and seal integrity through in vitro testing for 3–4 weeks. Prior to in vitro testing, devices were sterilized with 70 % ethanol during the fabrication process. After in vitro testing, devices were sterilized by submersion for 1 min in 70 % ethanol and allowed to dry. Devices were implanted in the vitreous chamber of the right eye of anesthetized New Zealand White rabbits. The left eye was left as an untreated control. All animal studies were performed following the ARVO statement for the use of animals in ophthalmic research, and the experimental protocols were approved by the University of California San Francisco Committee on
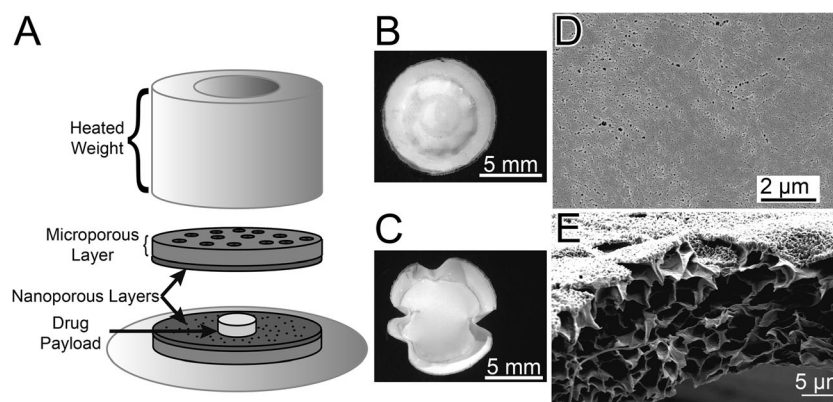

Fig. 1 Fabrication and morphology of nanoporous devices. **a** Schematic of the sealing process that uses a heated weight to seal two nanoporous films around a drug payload. (dimensions not to scale) **b** Sealed device containing a FITC-ranibizumab pellet. **c** Sealed device after hydration of the drug pellet, where osmotic pressure swells the device's internal reservoir. **d** SEM of the PCL film's nanoporous layer. **e** The nanoporous film in cross-section

774

Drug Deliv. and Transl. Res. (2016) 6:771–780

Animal Research. Devices were inserted into the vitreous cavity of one eye in adult New Zealand White female rabbits anesthetized by inhalation of 2–4 % isoflurane, and eyes received topical 0.5 % proparacaine drops, with 5 % povidone flush of the ocular surface. A conjunctival peritomy was performed to expose the sclera and then a 6-mm circumferential scleral incision was made 2 mm posterior to the corneal limbus with an microvitreoretinal blade. Devices were inserted into the vitreous cavity out of the visual axis using non-toothed forceps, with the flexibility of the polymer devices allowing partial device folding and entry through the incision. Any prolapsed vitreous gel was removed at the scleral surface with Westcott scissors and microsurgical sponges. The incision was closed with running sutures of 9–0 vicryl, with interrupted sutures to close the overlying conjunctiva. Subconjunctival antibiotic injections were given, along with topical erythromycin ointment. Rabbits were monitored for any indications of pain or irritation, such as eye redness, swelling, or eye guarding behavior to detect for any interference of the implanted devices upon vision.

FITC-ranibizumab concentration in the vitreous was assayed at weeks 1, 4, 8, and 12 following euthanasia ($n = 3$ rabbits at each time point). One rabbit was euthanized prior to week 6 due to complications from an infection unrelated to the device; IOP, adverse events, and device location information was not collected for that rabbit. Including the rabbit lost to complications, a total of 13 rabbits were used in the study. At each time point rabbit vitreous was completely sampled and devices were extracted. Vitreous was analyzed for FITC-ranibizumab concentration by size exclusion chromatography (see method below). Intraocular pressure (IOP), device location, and adverse events (cataracts, retinal damage, vitreous or aqueous chamber debris, edema, leakage) were tracked to monitor device safety and tolerability. A 30-degree prism lens was used in order to visualize the peripheral location of devices in the eye. Results are reported as plus/minus their standard deviations.

In vivo device safety and histology experiments

Two groups of four rabbits each were used to monitor device and drug effect on ocular tissues. One group was implanted with a FITC-ranibizumab-loaded device in the right eye with the same procedure as the in vivo elution experiments. The second group was implanted with a vehicle device without a drug payload. After 12 weeks, rabbits were euthanized and whole eyes were enucleated and fixed for histology using Davidson's solution over 24 h, followed by a transfer to 70 % ethanol. The fixed eyes were embedded in parafilm and representative sections were mounted on glass slides and stained with hematoxylin and eosin.

Post in vivo elution experiments and scanning electron microscopy

Following device extraction after in vivo release studies, devices were imaged using a dissection microscope to examine protein encapsulation and device integrity. Devices were then returned to in vitro elution conditions for 3–4 weeks using the methods described above. Following in vitro elution studies performed with recovered in vivo devices, the interior and exterior surfaces of the devices were examined by SEM as described above.

High performance size exclusion chromatography (HPSEC)

HPSEC was used to measure FITC-ranibizumab concentration for in vivo vitreous samples and to assess drug stability in both in vivo and in vitro devices. The remaining drug payload in each device after elution testing was used for HPSEC since the low concentration of eluted samples prevented HPSEC analysis. In brief, an isocratic buffer of 100 mM potassium phosphate (pH = 6.8) and 100 mM potassium chloride was run on an Agilent 1260 Infinity HPLC system with an Agilent Bio SEC-5 (5 μm, 4.6 × 300 mm) column at 0.4 mL/min for 70 min. Sample detection was performed via fluorescence (Ex 495 nm, Em 525 nm) on an Agilent 1260 FLD Spectra (model G1321B) and spectrometry (Abs 220, 280, and 495 nm) on an Agilent 1260 MWD VL (model G1365D). In vitro and in vivo samples were compared to a 10 mg/mL solution of FITC-ranibizumab stored at 37 °C as a control.

Quartz crystal microbalance (QCM)

Protein adsorption was measured using a Q-sense E4 instrument with 5 MHz gold Q-sense quartz crystal sensors spun-coated with a non-porous layer of PCL. PBS was flowed over sensors at a rate of 50 μl/min for 10 min at 37 °C to measure frequency baselines. Next, a 0.1 mg/mL ranibizumab solution was flowed over sensors at 50 μl/min for 30 min and 37 °C to measure protein adsorption.

Results

Device morphology

A pellet of fluorescein isothiocyanate (FITC) conjugated ranibizumab was encapsulated between two nanoporous films using heat sealing (Fig. 1a). The PCL films were approximately 20-μm thick and highly flexible. Assembled devices were 10 mm in diameter with a 6.5 mm diameter reservoir (Fig. 1b) and the heat-sealed perimeter maintained device integrity even with the osmotic pressure from drug pellet hydration (Fig. 1c). Scanning electron microscope (SEM) examination of the

device interior and cross-section shows the nanoporous layer and supporting meshwork of microporous PCL (Fig. 1d–e). The average ranibizumab payload of in vitro devices was 177 µg (±37 µg), with an average total formulation payload of 2.61 mg (±0.54 mg). The average ranibizumab payload of in vivo devices was 189 µg (±52 µg), with an average total device payload of 2.78 mg (±0.77 mg).

In vitro FITC-ranibizumab elution experiments

In vitro release of FITC-ranibizumab was recorded through 16 weeks and resulted in a biphasic release (Fig. 2a). A linear regression fit of the average normalized cumulative released data from day 1 to week 5 had a rate of 0.98 % per day ($y = 0.98 * x + 2.4$, $R^2 = 0.990$), while the linear fit for weeks 10–16 had a rate of 0.27 % per day ($y = 0.27 * x + 32.41$, $R^2 = 0.997$). On a monthly basis, these rates were 29 and 8.1 % of the initial payload released per month, respectively. The average residual payload at 16 weeks was 62.8 % (± 10.8 %) of the original loaded payload. The behavior of FITC-ranibizumab released at each time point showed a burst of release in the initial phase of the first 5 weeks, with a maximum at day 14 where 17 µg of FITC-ranibizumab was released in 1 week. This initial phase was followed by a gradually diminishing, second release phase up to week 16 where 2.3 µg of drug was released per week (Fig. 2b). The average
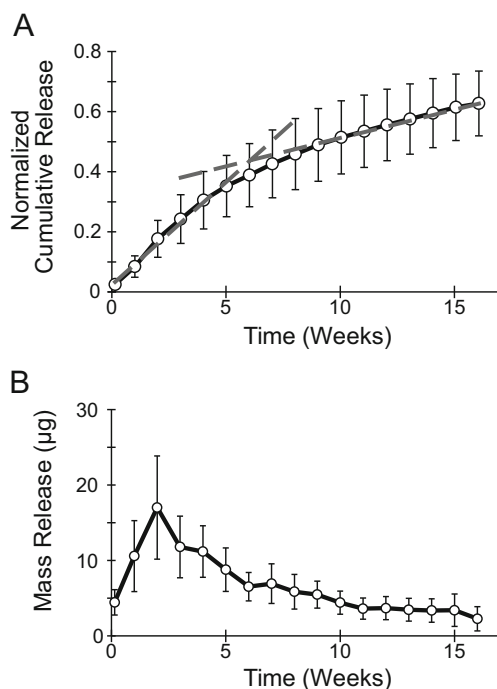

Fig. 2 In vitro release behavior of nanoporous devices. **a** Cumulative release of FITC-ranibizumab, normalized to the initial drug payload mass. The linear fit is shown for day 1 to week 5 ($R^2 = 0.990$) and weeks 10–16 ($R^2 = 0.997$). **b** Drug release shown as mass of FITC-ranibizumab released at each individual time point. $N = 17$ devices

initial release rate was 1.82 µg/day and decreased to an average terminal release rate of 0.56 µg/day. The maximum and minimum release rates for any 1-week period were 2.43 and 0.32 µg/day, respectively.

In vivo FITC-ranibizumab elution experiments

FITC-ranibizumab was detectable in the vitreous for 12 weeks of in vivo study. The highest concentration was at week 1 with an average concentration of 2.5 µg/mL (±1.3 µg/mL), while the remaining time points demonstrate extended release of FITC-ranibizumab through 12 weeks (Fig. 3a). At 12 weeks, ranibizumab concentrations were 0.83 µg/mL, while the combined average concentration over weeks 4, 8, and 12 was 0.96 µg/mL. Comparing device elution performance during in vitro testing both before and after in vivo implantation showed less than a 5 % difference in the rate of drug release (Fig. 3b).

Upon extraction, in vivo devices contained a visible yellow FITC-ranibizumab payload, were able to withstand swelling under osmotic pressure, and remained free of fibrous or cellular encapsulation for the implant duration (Fig. 3c–e). Examination of device surfaces using SEM revealed an intact internal nanoporous layer (Fig. 3f–g) and an intact external microporous surface (Fig. 3h). Some protein and salt crystal accumulation is evident in Fig. 3f; however, Fig. 3g shows an absence of large-scale protein adsorption. The few fissures observed in the nanostructured film (Fig. 3g) are an artifact of heating during SEM imaging. The external microporous layer is also free of large-scale protein residue (Fig. 3h).

In vivo safety profile

Devices were well-tolerated following implantation into the vitreous chamber of rabbit eyes (Fig. 4a). No statistical difference was found for intraocular pressure (IOP) between device eyes (12.0 ± 4.6 mmHg) and unimplanted control eyes (12.1 ± 5.3 mmHg) at sacrifice. Likewise, no statistical difference was found between device eye IOP pre-implantation (12.1 ± 4.7 mmHg) and at sacrifice (12.0 ± 4.6 mmHg). Adverse events observed in the in vivo elution study were iatrogenic cataracts in the device eye arm caused by surgical trauma to the lens during device implantation into the small confines of the rabbit eye (three vs. zero in the no-device control arm). No indications of pain or irritation, such as eye redness, swelling, or eye guarding behavior were observed. Device migration within the formed vitreous of the rabbit eyes was not seen, with stable location between implantation and sacrifice time points. Examination of device appearance in vivo showed a yellow, convex FITC-ranibizumab reservoir, a white margin of the sealed PCL perimeter around the reservoir, and an absence of fibrous encapsulation or vitreous debris (Fig. 4b). Histology was performed on sixteen eyes on the

776

Drug Deliv. and Transl. Res. (2016) 6:771–780

Fig. 3 In vivo behavior of nanoporous devices. **a** Average concentrations of FITC-ranibizumab measured in rabbit vitreous by size exclusion chromatography. The open circle at week 5.6 represents a single measurement. **b** FITC-ranibizumab in vitro elution before and after in vivo implantation, $n = 13$ devices, except † is $n = 3$ and ‡ is $n = 10$. **c**–**e** Example devices extracted after **c** 1 week, **d** 8 weeks, and **e** 12 weeks of in vivo implantation. **f**, **g** SEM of the internal nanoporous surface of a device reservoir after in vivo implantation. The *cracks* visible in **g** are artifacts associated with heating by the scanning electron beam. **h** SEM of the external surface of a device following in vivo implantation
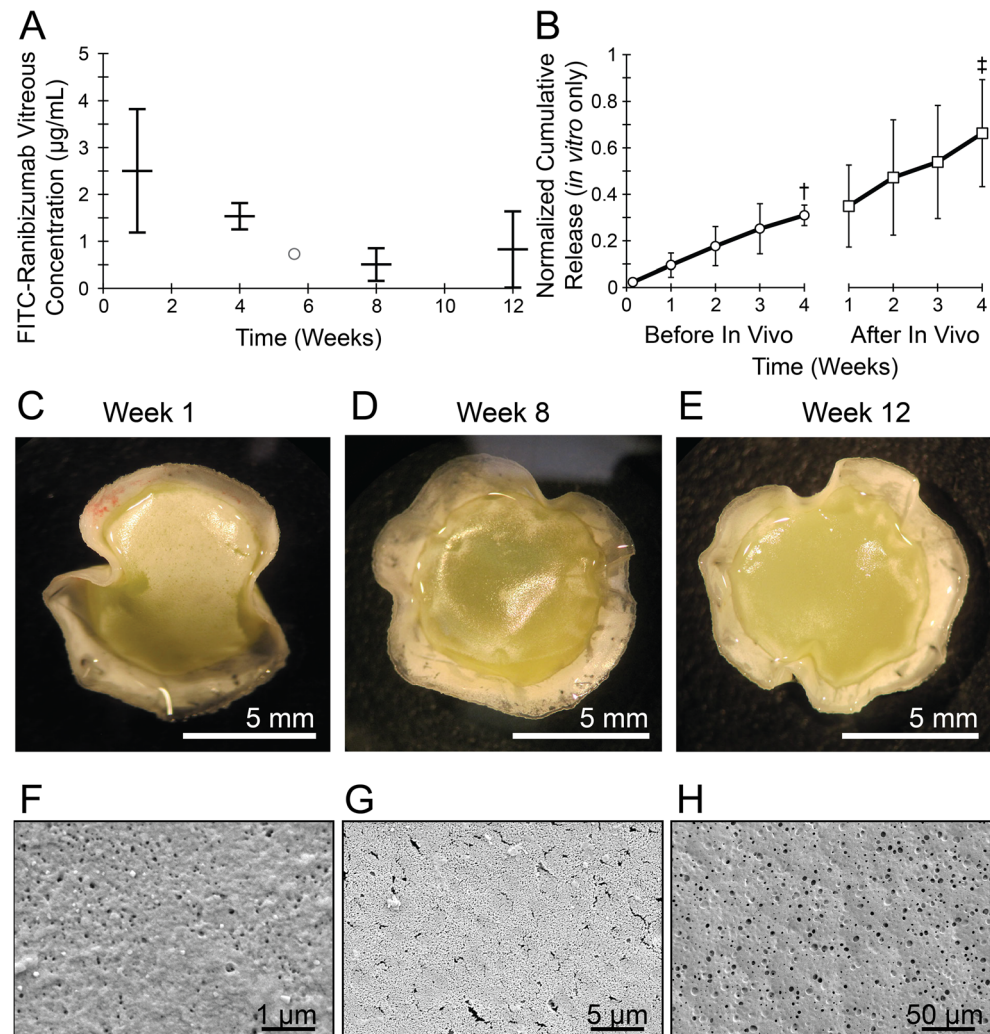
12th week; a histology-only device implantation study showed no retinal inflammation or morphology abnormalities between the four eyes receiving drug-loaded devices, the four eyes receiving empty devices, and the eight control eyes receiving no surgery (Fig. 4c–f).

Drug stability and protein adsorption

The relative stability of FITC-ranibizumab compared to controls was found to be 114 % (±14 %) for in vitro samples incubated for 16 weeks and 75.5 % (±27 %) for in vivo samples implanted in the rabbit vitreous between 1 and 12 weeks, including an additional 7 weeks of in vitro release testing. The control solution of FITC-ranibizumab maintained 93 % stability for 6 weeks at 37 °C, followed by a decay of up to 52 % stability at week 20. Protein aggregation was the mode of degradation for 91 % of the measured degradation in vivo and 100 % of the measured degradation in vitro, with any remainder being fragmentation. Four in vivo devices were excluded in this analysis because there was insufficient
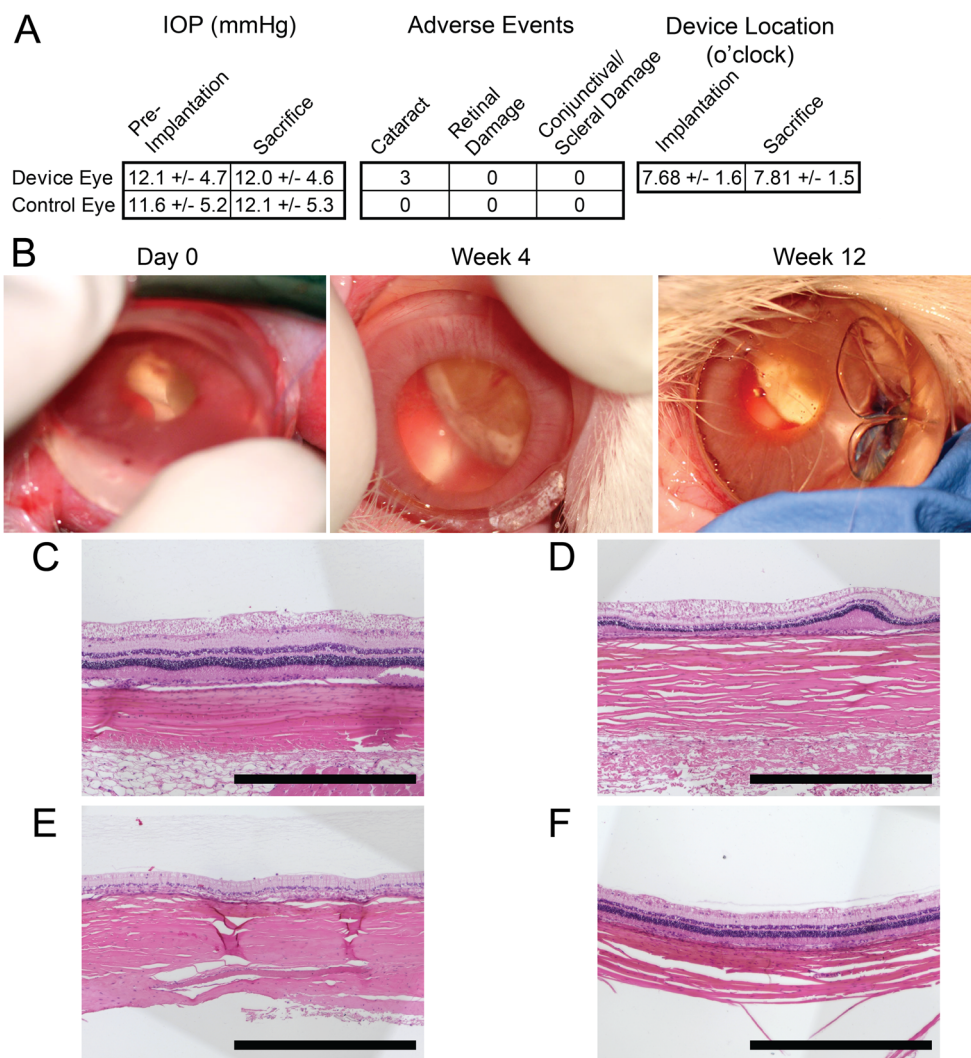
FITC-ranibizumab for HPSEC analysis following in vitro release testing of the recovered devices.

We evaluated the possibility of ranibizumab adsorption on the surface of PCL membranes as a potential means of sample loss or degradation. We used a QCM (sensitive to approximately 1 ng adsorbate per cm^2 of substrate) to obtain an estimate of the amount of protein adsorbed on the surface of a PCL thin film. Changes in frequency of the QCM correspond to changes in mass adsorbed to a surface. When ranibizumab was flowed over a bare gold surface, ample protein adsorption was observed (Fig. 5), whereas when ranibizumab was flowed over a gold substrate coated with a thin layer of PCL, no protein absorption was observed.

Discussion

The controlled release of ranibizumab from our nanoporous reservoir system represents a possible solution to the problem of sustained delivery of ranibizumab for retinal diseases. The elution behavior of the device shows a

Fig. 4 Device in vivo safety. **a**
IOP, count of adverse events, and
device location for in vivo devices
(*n* = 12). **b** Photographs of
implanted devices immediately
after implantation, after 4 weeks,
and after 12 weeks. The *bubble*
visible in week 12 is an artifact of
air under the contact prism lens
used for photographing devices.
c–f Hematoxylin-eosin staining of
rabbit retinae taken after 12 weeks
of FITC-ranibizumab-loaded
device or empty device
implantations, or no-surgery
controls. **c** Eye implanted with
drug-loaded device and **d**
companion eye. **e** Eye implanted
with empty device and **f**
companion eye. *Scale bar* is
500 μm

A

	IOP (mmHg)		Adverse Events			Device Location (o'clock)	
	Pre-Implantation	Sacrifice	Cataract	Retinal Damage	Conjunctival/Scleral Damage	Implantation	Sacrifice
Device Eye	12.1 +/- 4.7	12.0 +/- 4.6	3	0	0	7.68 +/- 1.6	7.81 +/- 1.5
Control Eye	11.6 +/- 5.2	12.1 +/- 5.3	0	0	0		

capability to retain and release a ranibizumab payload on the order of several months. The in vitro device performance shows sustained release over 16 weeks while only exhausting 62.8 % of its initial payload, suggesting a
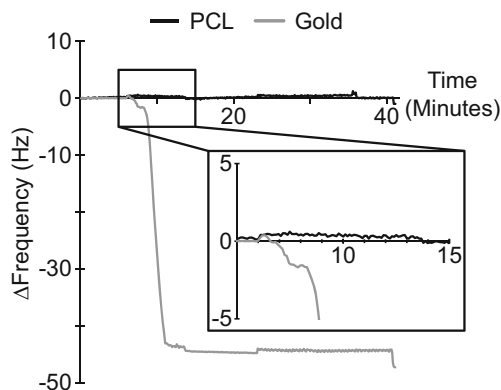

Fig. 5 Drug adsorption. QCM change in frequency for either a gold substrate or a PCL-coated gold substrate following exposure to ranibizumab solution

potential elution lifetime of approximately 25 weeks under in vitro conditions. In vivo elution studies on New Zealand White rabbits show therapeutically relevant concentrations of ranibizumab out to 12 weeks. For a ranibizumab delivery device, one can estimate relevant release rates to sustain therapeutic concentrations of long durations.

In previous studies, the half-life of ranibizumab in New Zealand White has been reported to be 2.9 days [35]. Using a one compartment model and assuming a constant rate of drug release, ocular concentrations can be approximated as:

$$C = C_{ss} * \left[1 - 2^{\wedge}\left(-t/t_{1/2} \right) \right]$$

where $t_{1/2}$ is time to reach half steady-state concentration and the steady-state concentration can be derived as C_{ss} = (rate of drug release)*$(t_{1/2})$/[(vitreous volume)*ln(2)].

Based on these assumptions, ocular concentrations will be within 95 % of steady-state concentrations after roughly 12.5 days. While a constant rate of release is an imperfect

778

Drug Deliv. and Transl. Res. (2016) 6:771–780

assumption for these devices, given our estimates for the time to approach a steady state, we can expect the in vivo concentrations measured at weeks 4, 8, and 12 will be representative of relevant long-term concentrations. Furthermore, using the average terminal release rate of 0.56 µg/day measured in vitro, reported ranibizumab clearance ($t_{1/2}$ = 2.9 days), and approximate rabbit vitreous volume (V_{vit} = 1.7 mL) [36], a steady-state concentration of 1.38 µg/mL is predicted. Variations between in vitro and in vivo release rates, saturated mechanisms for clearance of ocular ranibizumab, or imperfect estimates for vitreous volumes may contribute to the deviation between the predicted steady-state concentration and the average measured vitreous concentration of 0.96 µg/mL over weeks 4, 8, and 12.

Maintaining a steady-state concentration of ranibizumab allows the device to supply therapeutically effective concentrations of ranibizumab much longer than injections. The IC_{50} range for ranibizumab against VEGF is 11 to 27 ng/mL [37]. The pharmacokinetic parameters outlined in previous work in rabbits predict that an intraocular injection of 625 µg ranibizumab will cross this threshold after approximately 45 days (6.4 weeks) [38]. With this device we demonstrate vitreous concentrations of ranibizumab in excess of an order of magnitude (30–80×) higher than the IC_{50} through 12 weeks. Of note, such devices are able to achieve this time course with less than one-third the therapeutic payload of a bolus dose.

At the conclusion of in vivo studies, devices were recovered and release characteristics were reevaluated in vitro. Elution studies performed with recovered devices demonstrate continued constant-rate release, suggesting devices retain their elution capabilities even after weeks of exposure to rabbit vitreous. Examination of devices after extraction shows that device perimeter seals continue to retain osmotic pressure and there is no visible large-scale fibrous encapsulation by proteins or cells. This is expected given the eye's immune privileged nature and previous work with PCL in the eye demonstrating a lack of an inflammatory response [33]. High magnification SEMs of the device surfaces reveal a nanoporous surface with a mix of open and obstructed pores, possibly blocked by aggregates of ranibizumab formed in the highly concentrated interior of the device. It is possible that the adsorption of denatured protein aggregates and insoluble salts to nanopores slows drug release in vivo resulting in diminished release over time, but is reversed in the protein-free in vitro elution media. Another possible effect of any protein blockages could be manifested in the increase of the variation in the in vitro release rate between devices tested before and after in vivo testing (Fig. 3b).

Nanostructured PCL films have a history of biocompatibility when implanted in the vitreous [33]. Implantation of ranibizumab-loaded devices showed no significant increase in IOP over the 12 weeks of our study, along with no change in device location or signs of implant rejection. However, an increased occurrence of cataracts associated with device implantation can be attributed to the challenge of trauma-free surgical implantation in the small rabbit vitreous chamber relative to the size of the device. Because devices were designed for human treatment, the smaller vitreous cavity (1.7 mL vs. 4.7–5 mL) and the larger lens (thickness 6.7 vs. 3.89 mm) of this rabbit model compared to human anatomy are expected to contribute to an increased incidence of iatrogenic cataract formation [36, 39].

When compared to a free solution of FITC-ranibizumab after 16 weeks, encapsulated FITC-ranibizumab in in vitro devices at the same time point maintains a relative stability greater than 100 % as measured by HPSEC. This could be attributed to the difference in the hydrophobicity of their surroundings (PCL device vs. polypropylene tube), or exposure to the air interface for the FITC-ranibizumab solution. By comparison, encapsulated FITC-ranibizumab implanted in vivo had a lower stability relative to the free solution of FITC-ranibizumab at matching time points. It is important to note that our formulation of FITC-ranibizumab has not been optimized for long-term stability in a concentrated device reservoir. Future work will be needed to create an optimized formulation for long-term ranibizumab stability and release.

Optimization will also be needed for the sterilization process, with the most likely options being ethylene oxide exposure or gamma radiation used for sterilization before aseptic assembly. However, one potential drawback of ethylene oxide sterilization is the potential to alter the crystallinity of the PCL films [40]. Meanwhile, a risk of gamma radiation is increased PCL cross-linking and altered polymer surface morphology [41]. Future work will explore the effectiveness of both sterilization techniques and their impact on the performance of the device.

Conclusion

We have developed a nanoporous, thin-film, biodegradable device capable of eluting ranibizumab over the course of multiple months in the vitreous chamber of the eye. The device uses nanoporous PCL films to restrict the diffusion of ranibizumab out of a reservoir and has been shown to elute ranibizumab up to 16 weeks in vitro. Implantation of the devices into the vitreous chamber shows release of detectable amounts of ranibizumab out to 12 weeks with only partial occlusion of the nanopores and no presence of immune encapsulation. Extension of the presence of ranibizumab in the vitreous over the course of months with our device has the potential to improve compliance, reduce the cost of therapy for AMD treatment, and provide an option for long-term delivery of antibody-based drugs to the vitreous chamber of the eye.

Compliance with ethical standards All institutional and national guidelines for the care and use of laboratory animals were followed. All animal studies were performed following the ARVO statement for the use of animals in ophthalmic research, and the experimental protocols were approved by the University of California San Francisco Committee on Animal Research.

Conflict of interest Authors KDL, NAC, SDG, TSM, MK, EC, and MI declare that they have no conflict of interest.

Authors DAB, RBB, and TAD have founded a company based upon this technology.

References

1. Schwartz GF. Compliance and persistency in glaucoma follow-up treatment. Curr Opin Ophthalmol. 2005;16:114–21. doi:10.1097/01.icu.0000156139.05323.26.

2. Reardon G, Kotak S, Schwartz GF. Objective assessment of compliance and persistence among patients treated for glaucoma and ocular hypertension: a systematic review. Patient Prefer Adherence. 2011;5:441–63. doi:10.2147/PPA.S23780.

3. Ranta V-P, Mannermaa E, Lummepuro K, Subrizi A, Laukkanen A, Antopolsky M, et al. Barrier analysis of periocular drug delivery to the posterior segment. J Control Release. 2010;148:42–8. doi:10.1016/j.jconrel.2010.08.028.

4. Boddu SH, Gupta H, Patel S. Drug delivery to the back of the eye following topical administration: an update on research and patenting activity. Recent Pat Drug Deliv Formul. 2014:27–36. doi:10.2174/1872211308666140130093301.

5. Maurice DM. Drug delivery to the posterior segment : an update. Retin Today. 2013;47.

6. The CATT Research Group. Ranibizumab and bevacizumab for neovascular age-related macular degeneration. N Engl J Med. 2011;364:1897–908 .http://www.mendeley.com/research/ranibizumab-bevacizumab-neovascular-agerelated-macular-degeneration/. Accessed 14 Apr 2012

7. Heier JS, Brown DM, Chong V, Korobelnik JF, Kaiser PK, Nguyen QD, et al. Intravitreal aflibercept (VEGF trap-eye) in wet age-related macular degeneration. Ophthalmology. 2012;119:2537–48. doi:10.1016/j.ophtha.2012.09.006.

8. Varma R, Bressler NM, Suñer I, Lee P, Dolan CM, Ward J, et al. Improved vision-related function after ranibizumab for macular edema after retinal vein occlusion: results from the BRAVO and CRUISE trials. Ophthalmology. 2012;119:2108–18. doi:10.1016/j.ophtha.2012.05.017.

9. Nguyen QD, Brown DM, Marcus DM, Boyer DS, Patel S, Feiner L, et al. Ranibizumab for diabetic macular edema. Ophthalmology. 2012;119:789–801. doi:10.1016/j.ophtha.2011.12.039.

10. Ghasemi Falavarjani K, Nguyen QD. Adverse events and complications associated with intravitreal injection of anti-VEGF agents: a review of literature. Eye. 2013;27:787–94. doi:10.1038/eye.2013.107.

11. Townsend D, Reeves BC, Taylor J, Chakravarthy U, O'Reilly D, Hogg RE, et al. Health professionals' and service users' perspectives of shared care for monitoring wet age-related macular

12. degeneration: a qualitative study alongside the ECHoES trial. BMJ Open. 2015;5:e007400. doi:10.1136/bmjopen-2014-007400.

12. Amoaku W, Blakeney S, Freeman M, Gale R, Johnston R, Kelly SP, et al. Action on AMD. Optimising patient management: act now to ensure current and continual delivery of best possible patient care. Eye (Lond). 2012;26(Suppl 1):S2–21. doi:10.1038/eye.2011.343.

13. Busbee BG, Ho AC, Brown DM, Heier JS, Suñer IJ, Li Z, et al. Twelve-month efficacy and safety of 0.5 mg or 2.0 mg ranibizumab in patients with subfoveal neovascular age-related macular degeneration. Ophthalmology. 2013;120:1046–56. doi:10.1016/j.ophtha.2012.10.014.

14. Rawas-Qalaji M, Williams C-A. Advances in ocular drug delivery. Curr Eye Res. 2012;37:345–56. doi:10.3109/02713683.2011.652286.

15. Kang-Mieler JJ, Osswald CR, Mieler WF. Advances in ocular drug delivery: emphasis on the posterior segment. Expert Opin. Drug Deliv. 2014;5247:1–14. doi:10.1517/17425247.2014.935338.

16. Kuppermann BD, Blumenkranz MS, Haller JA, Williams GA, Weinberg DV, Chou C, et al. Randomized controlled study of an intravitreous dexamethasone drug delivery system in patients with persistent macular edema. Arch Ophthalmol. 2007;125:309–17. doi:10.1001/archopht.125.3.309.

17. Bhagat R, Zhang J, Farooq S, Li X-Y. Comparison of the release profile and pharmacokinetics of intact and fragmented dexamethasone intravitreal implants in rabbit eyes. J Ocul Pharmacol Ther. 2014;30:854–8. doi:10.1089/jop.2014.0082.

18. Kane FE, Burdan J, Cutino A, Green KE. Iluvien: a new sustained delivery technology for posterior eye disease. Expert Opin Drug Deliv. 2008;5:1039–46. doi:10.1517/17425247.5.9.1039.

19. Pardo-López D, Francés-Muñoz E, Gallego-Pinazo R, Díaz-Llopis M. Anterior chamber migration of dexametasone intravitreal implant (Ozurdex®). Graefe's Arch Clin Exp Ophthalmol. 2012;250:1703–4. doi:10.1007/s00417-011-1802-x.

20. Vela JI, Crespí J, Andreu D. Repositioning of dexamethasone intravitreal implant (Ozurdex®) migrated into the anterior chamber. Int Ophthalmol. 2012;32:583–4. doi:10.1007/s10792-012-9604-7.

21. Wai Ch'ng S, Padroni S, Banerjee S. Anterior vitreous displacement of the intravitreal dexamethasone implant (Ozurdex). Eye (Lond). 2014;28:238–9. doi:10.1038/eye.2013.270.

22. Kuno BN, Fujii S. Ocular drug delivery systems for the posterior segment : a review. Retin Today. 2012;54–59.

23. Kim YC, Chiang B, Wu X, Prausnitz MR. Ocular delivery of macromolecules. J Control Release. 2014;190:172–81. doi:10.1016/j.jconrel.2014.06.043.

24. Taluja A, Youn YS, Bae YH. Novel approaches in microparticulate PLGA delivery systems encapsulating proteins. J Mater Chem. 2007;17:4002. doi:10.1039/b706939a.

25. Sinha VR, Trehan A. Biodegradable microspheres for protein delivery. J Control Release. 2003;90:261–80 .http://www.ncbi.nlm.nih.gov/pubmed/12880694

26. Nadarassan DK. Sustained release of bevacizumab (Avastin) from BioSilicon. Invest Ophthalmol Vis Sci. 2014;55:1950.

27. Owens G, Williams S, Herlihy K, Tully J, Verhoeven RS, Navratil T, et al. Establishing in vivo to in vitro correlations for the rate of release of bevacizumab from extended release formulations. Invest Ophthalmol Vis Sci. 2015;56:236.

28. R.G. Rubio. Long-acting anti-VEGF delivery. Retin Today. 2014;78–80.

29. Mitragotri S, Burke PA, Langer R. Overcoming the challenges in administering biopharmaceuticals: formulation and delivery strategies. Nat Rev Drug Discov. 2014;13:655–72. doi:10.1038/nrd4363.

30. Wu F, Jin T. Polymer-based sustained-release dosage forms for protein drugs, challenges, and recent advances. AAPS PharmSciTech. 2008;9:1218–29. doi:10.1208/s12249-008-9148-3.

780

Drug Deliv. and Transl. Res. (2016) 6:771–780

31. Bernards DA, Desai TA. Nanotemplating of biodegradable polymer membranes for constant-rate drug delivery. Adv Mater. 2010;22: 2358–62. doi:10.1002/adma.200903439.

32. Bernards DA, Lance KD, Ciaccio NA, Desai TA. Nanostructured thin film polymer devices for constant-rate protein delivery. Nano Lett. 2012;12:5355–61. doi:10.1021/nl302747y.

33. Bernards DA, Bhisitkul RB, Wynn P, Steedman MR, Lee O-T, Wong F, et al. Ocular biocompatibility and structural integrity of micro- and nanostructured poly(caprolactone) films. J Ocul Pharmacol Ther. 2013;29:249–57. doi:10.1089/jop.2012.0152.

34. Silva-Cunha A, Fialho SL, Naud M-C, Behar-Cohen F. Poly-ε-caprolactone intravitreous devices: an in vivo study. Investig Opthalmology Vis Sci. 2009;50:2312. doi:10.1167/iovs.08-2969.

35. Gaudreault J, Fei D, BEYER JC, Ryan A, Rangell L, Shiu V, et al. Pharmacokinetics and retinal distribution of ranibizumab, a humanized antibody fragment directed against VEGF-A, following intravitreal administration in rabbits. Retina. 2007;27:1260 .http://journals.lww.com/retinajournal/Abstract/2007/11000/Pharmacokinetics_and_Retinal_Distribution_of.18.aspx. Accessed 18 Apr 2011

36. Missel PJ. Simulating intravitreal injections in anatomically accurate models for rabbit, monkey, and human eyes. Pharm Res. 2012;29:3251–72. doi:10.1007/s11095-012-0721-9.

37. Genentech Inc. Prescribing Information for Lucentis® (Ranibizumab). 2006.

38. Gaudreault J, Fei D, Beyer JC, Ryan A, Rangell L, Shiu V, et al. Pharmacokinetics and retinal distribution of ranibizumab, a humanized antibody fragment directed against VEGF-A, following intravitreal administration in rabbits. Retina. 2003;27:1260–6. doi:10.1097/IAE.0b013e318134eecd.

39. Vézina M. Assessing ocular toxicology in laboratory animals. In: Weir AB, Collins M, editors. Assess. Ocul. Toxicol. Lab. Anim. Totowa: Humana Press; 2013. p. 1–21. doi:10.1007/978-1-62703-164-6.

40. Weir NA, Buchanan FJ, Orr JF, Farrar DF. Influence of processing and sterilisation on properties of poly-ε-caprolactone. Plast Rubber Compos. 2003;32:265–70. doi:10.1179/146580103225010264.

41. Cottam E, Hukins DWL, Lee K, Hewitt C, Jenkins MJ. Effect of sterilisation by gamma irradiation on the ability of polycaprolactone (PCL) to act as a scaffold material. Med Eng Phys. 2009;31:221–6. doi:10.1016/j.medengphy.2008.07.005.